

BPEC: An R Package for Bayesian Phylogeographic and Ecological Clustering

Ioanna Manolopoulou

University College London
UK

Axel Hille

Institute of Applied Statistics Dr Jörg Schnitker
Germany

Abstract

BPEC is an R package for Bayesian Phylogeographic and Ecological Clustering which allows geographical, environmental and phenotypic measurements to be combined with DNA sequences in order to reveal clustered structure resulting from migration events. DNA sequences are modelled using a collapsed version of a simplified coalescent model projected onto haplotype trees, which subsequently give rise to constrained clusterings as migrations occur. Within each cluster, a multivariate Gaussian distribution of the covariates (geographical, environmental, phenotypic) is used. Inference follows tailored Reversible Jump Markov chain Monte Carlo sampling so that the number of clusters (i.e., migrations) does not need to be pre-specified. A number of output plots and visualizations are provided which reflect the posterior distribution of the parameters of interest. **BPEC** also includes functions that create output files which can be loaded into Google Earth. The package commands are illustrated through an example dataset of the polytypic Near Eastern brown frog *Rana macrocnemis* analysed using **BPEC**.

Keywords: statistical phylogeography, biogeography, population genetics, Bayesian computation, R.

1. Introduction

Phylogeography (and population genetics), a term coined by [Avise et al. \(1987\)](#) to refer to the analysis of genealogies obtained from mtDNA sequences in relation to the geographic distribution of species, has seen a surge of methods in the past 20 years which address a wide variety of different questions, under a range of different assumptions and with varying model complexity. The breadth of existing methods is not only reflective of the challenges that phylogeographic data pose, but also of the multitude of scientific questions that these data might hold the answer to. A few relatively recent reviews, [Bloomquist et al. \(2010\)](#); [Ronquist and Sanmartín \(2011\)](#); [Knowles and Maddison \(2002\)](#); [Knowles \(2009\)](#), give an overview and comparison of many of the existing approaches.

Many of the methods do not use geographical information explicitly so rely on population genetics modelling. For example, [Pritchard et al. \(2000\)](#) (and subsequent papers) developed a method called **STRUCTURE** for analysing gene-flow among sub-divided populations, a software which infers population structure purely from genotype data through a Latent Dirichlet Allocation model. Population subdivisions are assessed on the basis of multi-locus allele frequencies which are directly learnt from data. More recently, [Jombart et al. \(2010\)](#) developed

DAPC, a principal-components alternative to **STRUCTURE** which can computationally efficiently deal with large amounts of data. Fully model-based extensions of spatially-explicit inferences of population structure such as **GENELAND** (Guillot *et al.* 2005, and subsequent papers) assume that the spatial domain occupied by the inferred clusters can be approximated by a small number of polygons based on Voronoi tessellations. Drawing inferences about these cluster domains (and thus about cluster membership) amounts to inferring the location and cluster memberships of the polygons.

Another population genetics approach is implemented in the software **Migraine** which uses coalescent algorithms for maximum likelihood analysis of population data, accounting for various forms of isolation-by-distance models of population structure (Leblois *et al.* 2014). An alternative method combines graph theory with topological congruence in order to characterise geographical structure in the R package **popgraph** (Dyer and Nason 2004).

In order to study population history together with past population structure, Templeton (1998) developed a method for inferring phylogeographic structure using DNA sequences and geographical locations of observations. The method uses a parsimonious neighbour-joining haplotype tree in which two haplotypes are joined by an edge if and only if a quantity called “probability of parsimony” exceeds 95% for that edge. The haplotype network is then analysed based on an inference key (Templeton 2004; Panchal and Beaumont 2007) in order to infer phylogeographic structure and history. Nested Clade Phylogeographic Analysis can provide very specific conclusions about the phylogeographic hypotheses supported by the data, but is not model-based and thus its reliability and quantification of uncertainty has come into question (Beaumont *et al.* 2010).

In more recent years, fully model-based inference has allowed the study of migration via phylogeographic inference on datasets from known population geographical structure (see Sanmartín *et al.* 2010). Sanmartín *et al.* (2010) define a fully flexible migration model in order to infer phylogeographic history, allowing for different rates of migration across different population subgroups, taking into account geographical distance.

An alternative to a discrete subdivided population was developed by Lemey *et al.* (2009); Bielejec *et al.* (2011) using fully model-based phylogeographic inference, which departed from the island migration model to assume a diffusion for the geographical migration of nodes on a phylogenetic tree, so that evolution and migration events occur in a continuous-time framework.

Ranjard *et al.* (2014) for the first time estimated the joint effects of limited dispersal and ecological competitive exclusion in a statistical phylogeographic framework and implemented their model in the R package **phyloland**. It defines a landscape as a set of vacant locations that are colonized through a series of dated dispersal events. According to this approach, dispersal is mapped on the genealogy, each internal node corresponding to a specific dispersal event. Bayesian stochastic simulation algorithms are used to sample the model for inference of the parameters: σ , the standard deviation of the normal distribution for the dispersal kernel, λ , the probability of migrating to an occupied location, τ , the number of dispersal events per unit of time, and the geographic locations at the internal nodes of the phylogeny.

Here we present another novel R package (R Core Team 2015) available from the Comprehensive R Archive Network at <http://CRAN.R-project.org/package=BPEC> which automates Bayesian Phylogeographic and Ecological Clustering (BPEC) analysis (Manolopoulou *et al.* 2011; Manolopoulou and Emerson 2012). **BPEC** is a model-based approach which assumes

that population substructure is the result of individual migration events and thus infers geographical population clusters, while also admitting a model for the evolutionary history. The key function of **BPEC** inputs non-recombinant DNA sequences and geographical locations, as well as any additional covariates available, such as temperature or phenotypic characteristics in order to identify population clusters as a result of migration. The results of the analysis provide estimates on the number of migration events without pre- defining its numbers, geographical distribution of clusters, ancestral locations and clustered tree structure. Aside from providing estimates for the quantities of interest, **BPEC** also provides measures of uncertainty of the conclusions and functions for post-processing. Finally, **BPEC** is supplemented with various visualization tools interfacing with Google Earth TM to aid interpretation. In Section 1, we discuss different approaches and challenges in statistical phylogeography. We follow by presenting the **BPEC** model in Section 2, along with corresponding Bayesian computation methods (Section 3). The R user interface is presented in Section 4, together with examples from the application of **BPEC** on a dataset of the eastern lineages of polytypic Near Eastern brown frogs, *Rana macrocnemis* (Boulenger, 1885), from the Caucasus region (Tarkhnishvili et al. 2001). The output is analysed and interpreted in Section 5 as an example of the type of conclusions that can be drawn using **BPEC**. The paper concludes with a short discussion in Section 6.

2. Model

The aim of phylogeographical analyses through **BPEC** is to combine sequence data \mathcal{S} with geographical and ecological data \mathcal{Y} in order to draw conclusions about the geographically clustered structure consistent with the evolutionary history of the organisms of interest. **BPEC** combines an evolutionary model for the DNA sequences through a haplotype tree together with a geographical model representing migrations forming clusters into a fully model-based framework.

2.1. Haplotype tree model

Evolutionary modelling of DNA sequences is complex and approaches range from simple and elegant such as the vanilla coalescent (Kingman 1982) to complex with intractable likelihood forms (Cornuet et al. 2014). Questions such as the validity of a constant (or effectively constant) population size, independent nucleotide mutations, constant mutation across sites, time-dependence, presence of natural selection pressure, all play a role in defining an appropriate evolutionary model and have led to different extensions of the basic model (Wakeley 2013; Hein et al. 2004). In our case, the typical datasets at hand range around a few hundred mtDNA sequences with length 100-10,000 nucleotides. Given the short length of the sequences, it is common that haplotypes (i.e., distinct sequences) appear repeatedly in the data. As a result, the nucleotide data are noisy and often too weakly informative to allow for very complex models.

There are two main tree representations of evolutionary histories. The first is via a coalescent tree (with or without mutations); the second is via cladograms, haplotype trees or networks. A coalescent tree is plotted against time and thus explicitly characterizes the most recent common ancestor (TMRCA). An example of a coalescent tree with mutations is shown in Figure 1: the tips represent observed sequences and black circles indicate mutations. As

time progresses, both mutation and coalescence events occur. In contrast, haplotype trees are plotted against number of mutations, so only implicitly carry information about time. The haplotype tree corresponding to the coalescent tree of Figure 1 is shown in Figure 2. Given a haplotype tree, an evolutionary model is subsequently needed to allow us to draw inferences about the root haplotype within a given tree. However, probabilities of evolutionary histories over rooted haplotype trees are not readily available; models such as the coalescent with mutations are, instead, available (Ethier and Griffiths 1987).

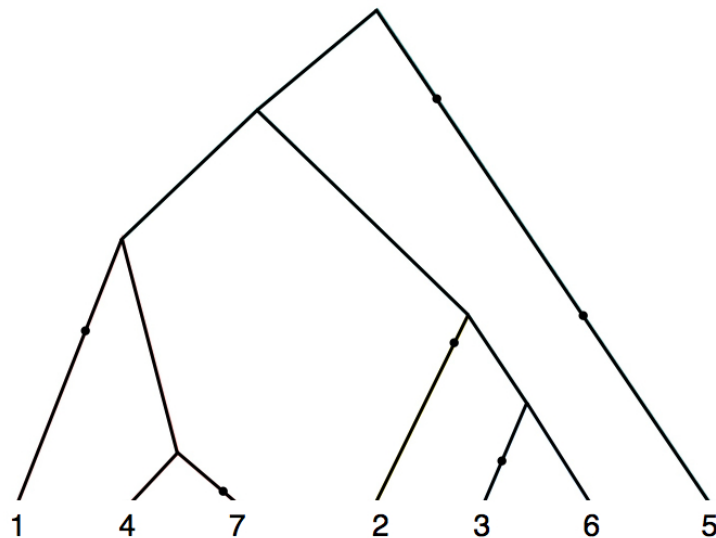


Figure 1: An example of a coalescent tree with mutations for 7 observed sequences including mutations; black dots represent mutations. Time evolves from top to bottom.

In the current context, there is a subtle complication because the tree may be unidentifiable given repeated observations of the same haplotype; for example, in Figure 1, observations 4 and 6 correspond to the same haplotype. This happens because, in the limited length of nucleotide sequences observed, not enough mutations are present compared to the number of sequences collected. This means that these 2 observations could be switched without having any effect on the likelihood of the genetic sequences. Observations may be distinct via the geographical or ecological information associated to each one. Aside from identifiability issues, exploring the space of equivalent trees requires cycling through a complex combinatorial object which quickly becomes computationally cumbersome. Collapsing the sequences onto haplotypes and switching from coalescent to haplotype trees allows us to get around this issue, reducing the space of possible trees. The coalescent tree from Figure 1 is now represented through the haplotype tree shown in Figure 2; sequences 4 and 6 are represented by the same node in the tree.

In order to draw inferences about the haplotype tree, approaches can be fully model-based (Felsenstein 1983; Huelsenbeck and Ronquist 2001; Drummond et al. 2012), parsimony-based through the underlying tree (Rzhetsky and Nei 1993; Desper and Gascuel 2002), or purely phenetic such as neighbour-joining or median-joining (Atteson 1999; Gascuel and Steel 2006). **BPEC** combines parsimonious approaches within a model-based framework. Although an infinite set of haplotype or coalescent trees could be consistent with the sequence data \mathcal{S} ,

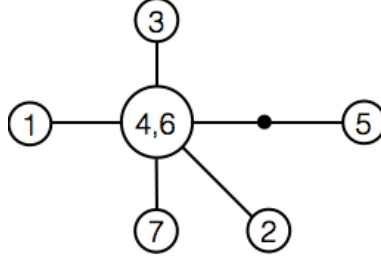


Figure 2: The corresponding haplotype tree of Figure 1, where edges represent single effective mutations. The black dot represents an unobserved intermediate sequence. Note that sequences 4 and 6 correspond to the same haplotype.

BPEC uses relaxed parsimony to reduce it to a finite set of ‘plausible’ trees Ω represented via a graph (Manolopoulou and Emerson 2012). The relaxed parsimony is defined by a threshold d_s representing parsimony relaxation. Briefly, haplotypes are connected by an edge if they are a single mutation apart. When two groups of haplotypes are disconnected (with minimum mutation distance d_{min}), then any connection path with length up to $d_{min} + d_s$ is considered. The exact details of how to obtain Ω from \mathcal{S} for a given d_s can be found in algorithm A of Manolopoulou and Emerson (2012). This algorithm constructs a set of ‘realistic’ trees by cumulatively adding intermediate sequences following a relaxed parsimony assumption defined by the user-specified parsimony relaxation parameter d_s . In general, larger values of d_s (up to a maximum value) yield more inclusive (and hence realistic) sets Ω , but the choice of d_s is often limited by computational power. For a fixed d_s , this algorithm inputs the DNA sequences at hand, and outputs a sequence network, including loops. The true haplotype tree is then assumed to be one of the minimum spanning trees of this graph with equal probability and can be obtained through the breaking of loops.

A haplotype tree encodes less information than a coalescent tree with mutations. Firstly, a haplotype tree only encodes time through number of mutations. Secondly, it does not automatically define an ordering of events, starting from a root down to tips. Even a rooted (i.e. one where the ancestral haplotype is specified) haplotype tree imposes only a partial ordering to the set of past mutation and coalescence events. Calculating probabilities over rooted haplotype trees therefore requires summing over all possibilities and orderings of past events given a temporal model; an example of possible orderings is shown in Appendix 7.1. We denote a temporal ordering of events as \mathcal{O} , where $\mathcal{O}_{r,T}^{\mathcal{S}}$ denotes the set of all temporal orderings consistent with data \mathcal{S} given a root r and tree T and assume that any temporal ordering of events is equally likely a priori. Although in the infinite discrete set of temporal orderings this prior distribution is somewhat meaningless, conditionally on observed data (which restricts the possible trees to the space Ω) it provides the following posterior probabilities for the root r and tree T :

$$\mathbb{P}(r, T \mid \mathcal{S}) = \frac{|\mathcal{O}_{r,T}^{\mathcal{S}}|}{\sum_{r,T} |\mathcal{O}_{r,T}^{\mathcal{S}}|},$$

where $|\cdot|$ denotes the size of the set. Similarly,

$$\begin{aligned}\mathbb{P}(r \mid T, \mathcal{S}) &= \frac{|\mathcal{O}_{r,T}^{\mathcal{S}}|}{\sum_r |\mathcal{O}_{r,T}^{\mathcal{S}}|}, \\ \mathbb{P}(T \mid r, \mathcal{S}) &= \frac{|\mathcal{O}_{r,T}^{\mathcal{S}}|}{\sum_T |\mathcal{O}_{r,T}^{\mathcal{S}}|}.\end{aligned}$$

This model naturally takes into account the total number of combinations of splitting and coalescence events. Note that this model disregards the relative probability of coalescence versus mutations, essentially assuming that at every time point either are equally likely. The model can be extended to introduce a mutation rate θ (at the expense of computational complexity) which is simultaneously learnt and is used to refine the posterior probabilities of each tree.

Although the haplotype tree model described provides a way of assigning posterior probabilities of haplotypes being ancestral, these need to be linked up to sampling locations in order to infer the most ancestral location. **BPEC** assigns probabilities to each location based on the haplotypes observed in each one. For each posterior sample, if the root haplotype is observed, then each observed sequence that corresponds to that haplotype contributes equally to a location being ancestral; in other words, each location will be likely to be ancestral with probability equal to the proportion of root haplotypes that were sampled in it. If the root haplotype is not observed (i.e., is extinct in the entire dataset), then the oldest observed haplotypes (down each clade stemming from the root) are considered equally likely to be the ‘most ancestral’ and thus each observation of one of these haplotypes contributes equally to the probability of each sampling location being ancestral. An example of this is shown in Figure 3. A key feature of this approach is that the number of sampled observations per location do not play a role; instead the distribution of haplotypes within it determine whether the location is ancestral. This is to circumvent issues of wide sampling variability across locations.

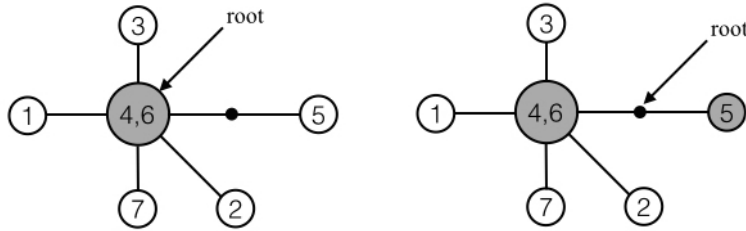


Figure 3: Two possible root scenarios. In the left-hand panel, the root haplotype (shown in grey) is observed and thus any location will be ancestral according to the proportion of observations of haplotype 4 it contains. In the right-hand panel, the root haplotype is not observed; the two oldest descendants (shown in grey) are then haplotypes 4 and 5. Any location will then be ancestral proportionally to the number of copies of haplotypes 4 or 5 that it contains.

2.2. Clustering model

The two main ingredients required to infer migration events given a tree are a model for constructing constrained clusterings conditionally on a haplotype tree, along with a model for the distribution of data within each cluster. A key assumption in our model is that new clusters are formed through migration of a single individual founding a new colony/cluster (De Iorio and Griffiths 2004a,b). All of its descendants subsequently belong to the new cluster, unless they migrate again. Given a known tree representing the genealogy, possible clusterings of the data are thus constrained by the tree while at the same time informed via the distribution of the observations for each individual. This is better understood through an example: in Figure 4, originally there was only the green cluster. A migration event of a haplotype identical to the root then led to the formation of the red cluster, similarly with the yellow and light blue, resulting in entire clades representing clusters. We would naturally expect all observations belonging to each cluster to also be geographically clustered accordingly.

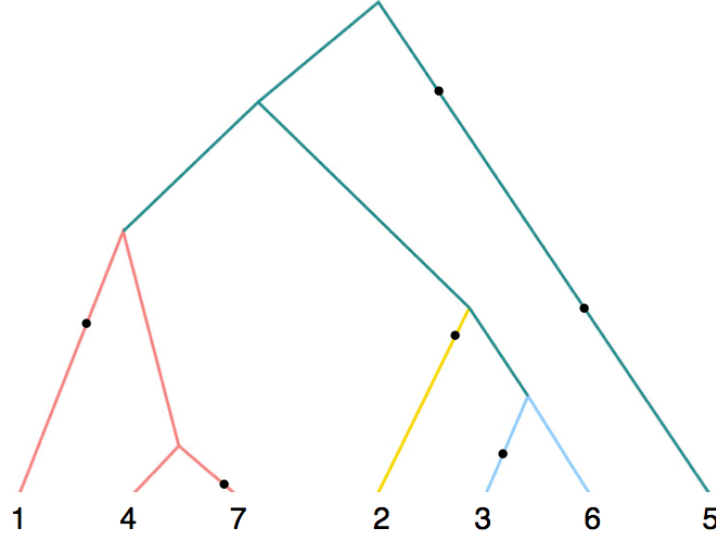


Figure 4: A subdivided example of the coalescent tree shown in Figure 1, where colour corresponds to population cluster and black dots represent mutations.

The coalescent tree determines a set of constrained clusterings which are feasible through migration events. For example, observation 2,3 and 6 in Figure 4 could have formed a single cluster together, but 6,7 could not. Although intuitive when viewed on the coalescent tree, the corresponding constrained clusterings defined on the collapsed haplotype tree are slightly more complicated since repeated observations of the same node/haplotype could belong to different clusters. In the collapsed haplotype network shown in Figure 5, all clustered nodes must be directly connected within their cluster. However, it is also possible that, although haplotype 4/6 migrated, only haplotypes in the light blue cluster were observed (in Figure 4, imagine that sequence 4 were not observed). Then the 4/6 haplotype would be fully light blue, but adjacent 1 and 7 would be pink. For simplicity, we shall refer to haplotype 4/6 as haplotype 4 from now on.

Formally, conditionally on a haplotype tree, the clustering model is defined as follows. We

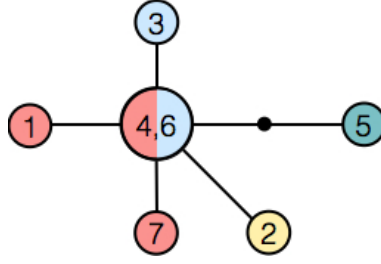


Figure 5: The clustered haplotype tree corresponding to the subdivided coalescent tree of Figure 4 where colour corresponds to cluster and size of node to the number of individuals sampled with each sequence. Haplotypes are numbered according to the input NEXUS file. Edges represent single effective mutations and black dots represent unobserved intermediate haplotypes.

denote the set of distinct haplotypes in the sequence set \mathcal{S} (of size N) as $\mathcal{H} = \{H_1, \dots, H_n\}$ with size n , and use $|H_i|$ to denote the number of copies of haplotype H_i observed in the data. Let K denote the number of migrations, which is itself allowed to vary. Each migration event is associated with a haplotype which migrated, denoted as $\mathbf{m} = \{m_1, \dots, m_K\}$. Although colonisation events happen in order, here we do not model the events temporally, so the order of \mathbf{m} is irrelevant. Note that the haplotypes in this list need not be distinct, as two different copies of the same haplotype may have colonised, or a single sequence may have colonised twice. The set of colonies/clusters with which each migrating haplotype is associated is denoted by $\mathcal{C}(m_k)$, $k = 1, \dots, K$; in the example above, $K = 3$, $\mathbf{m} = \{4, 4, 4\}$ and $\mathcal{C}(4) = \{\text{blue, yellow, pink, green}\}$, since all migrations were of the same haplotype. This means that, in general, the sample space of \mathbf{m} has size $n^K/K!$.

Conditionally on a set of migrating haplotypes, the space of constrained clusterings is then such that all observations of that haplotype must belong to one of the corresponding clusters $\mathcal{C}(m_k)$ (i.e., either the original cluster or the one which was a result of migration). Equivalently, all adjacent haplotypes must also belong to one of these clusters (unless one of them also migrated, and so on).

Once the clustering has been established, the geographical and ecological observations Y_i , $i = 1, \dots, N$ in each cluster c_i are Normally distributed with mean μ_c and variance Σ_c , such that

$$Y_i \sim N(\mu_{c_i}, \Sigma_{c_i}), \quad i = 1, \dots, N, \quad (1)$$

where c_i denotes the cluster of observation i .

To complete the model, prior distributions are defined on the model parameters. The number of migrations is assumed to be uniform between 0 and K_{\max} (corresponding to 1 and $K_{\max} + 1$ clusters). Other prior distributions (e.g. Poisson) could be used instead, but we do not explore this direction here. The $|m_k|$ observations of each of the migrating haplotypes m_k are each assigned uniformly to one of the clusters in \mathcal{C}_k , similarly with the $\deg(m_k)$ clades connected to it (where degree represents the number of edges connected to node m_k), so the prior probability of each clustering conditional of the migrating haplotypes (and their clusters) is

simply a combinatorial coefficient.

$$\begin{aligned}
K &\sim \mathcal{U}\{0, \dots, K_{\max}\}, \\
\mathbf{m} \mid \mathcal{S} &\sim \text{Multinomial}\{|H_1|, \dots, |H_n|\} \\
\text{and } p(\mathbf{c} \mid \mathbf{m}, T) &= \prod_{k=1}^K \left(\frac{1}{|\mathcal{C}_k|} \right)^{|m_k| + \deg(m_k)}
\end{aligned} \tag{2}$$

The means and variances of each clustering are assigned different priors for the longitude-latitude versus the remaining covariates:

$$\begin{aligned}
\Sigma_{k,(1:2,1:2)} &\sim \mathcal{IW}(\gamma, \psi \mathbb{I}_2), \quad k = 1, \dots, (K_{\max} + 1), \\
\Sigma_{k,(3:d)} &\sim \mathcal{IG}(\gamma, \psi), \quad k = 1, \dots, (K_{\max} + 1), \\
\gamma &\sim \mathcal{U}\{4, \dots, g\}, \\
\boldsymbol{\mu}_k \mid \Sigma_k &\sim \mathcal{N}(\mathbf{0}, V), \quad k = 1, \dots, (K_{\max} + 1),
\end{aligned} \tag{3}$$

and we assume that any off-diagonal entries of Σ_k in dimensions $3 : d$ are 0. By convention, the first two coordinates of Y always represent latitude and longitude, normalised such that the mean of both is zero and the average (between latitude and longitude) variance 1, using the same normalising factor for both latitude and longitude to reflect the isotropy of the two dimensions. The remaining coordinates correspond to environmental or phenotypic characteristics (if available), which are normalised to sample mean 0 and marginal variance 1. We impose uncorrelated environmental/phenotypic characteristics by forcing the covariance matrices to be 0 on any off-diagonal entries except for the one corresponding to longitude-latitude. This is because the concentration parameter γ of an Inverse Wishart needs to be at least as $d_{\Sigma} + 2$ in order to be well-defined, where d_{Σ} is the dimension of the covariance matrix modelled. In our case, if we model the entire covariance matrix through an Inverse Wishart, γ would be forced to a minimum of $3 + d$, which (for moderate d) corresponds to low prior variance and can be too restrictive. We thus restrict the Inverse-Wishart prior for the geographical covariates only and place independent Inverse-Gamma priors on the remaining diagonal elements of Σ_k .

Perhaps the most important prior distributions here are the ones relating to the shape Σ of each cluster, namely the parameters of the Inverse-Wishart prior γ and ψ , as these define the prior belief of the spread of each cluster. Although the parameter γ is allowed to vary and hence can adapt depending on information from the data, nevertheless too large or too small values of ψ (corresponding to a prior belief of geographically widely spread versus tiny clusters) will have an impact on the posterior inference. The default setting in **BPEC** is that clusters are a priori expected to span about 30% of the total range.

3. Bayesian computation in BPEC

The entire model consists of the model of the root and tree posterior distribution together with the distribution of the migration and clustering model. Inferences are drawn simultaneously, such that we can borrow information from the tree to the migration parameters and vice versa. The complexity of this phylogeographic model implies that drawing inferences about the posterior distribution of the parameters is challenging. We proceed via tailored Markov

chain Monte Carlo (MCMC) using a combination of adaptive proposals, auxiliary variables and data-driven proposals. This is especially crucial for the clustering, which here is restricted to tree-based clusterings, since the space of clusterings is vast and discrete without natural local moves.

3.1. Markov chain Monte Carlo sampler

The Markov chain Monte Carlo sampler alternates between updates of the tree parameters and the clustering parameters. We adopt a scheme whereby updates of parameters are performed at varying frequencies, reflecting the difficulty of accepting or rejecting a move and allowing both local and global exploration of the parameter space. Four different updates are described below, which are then combined into a sampler at varying frequencies.

The tree T , root r , colonised haplotypes \mathbf{m} , clustering \mathbf{c} and cluster means μ and variances Σ .

1. Conditionally on a given tree T , propose to change the root along with a mutation history. Accept or reject the proposed root and mutation history.
- 2a. Conditionally on the root r , propose a new tree T and mutation history uniformly.
- 2b. Conditionally on the proposed tree T propose to change one of the colonised haplotypes in \mathbf{m} .
- 2c. Conditionally on the colonised haplotypes, propose to change the set of clusterings \mathbf{c} along with the means μ and variances Σ of each cluster.
- 2d. The proposed tree topology and history, root, clustering and means and variances are accepted or rejected together. However, steps (2a), (2b) and (2c) need not all occur at the same time. Specifically, steps (2a-b) are only performed (roughly) every 5th iteration.
3. Conditionally on a given clustering, update the cluster means conditionally on all other parameters, and subsequently the sample covariance conditionally on all other parameters.
4. Propose to increase or decrease the number of clusters. Then propose to add or subtract a colonised sequence, then set of clusterings together with means and variances of each cluster. Accept or reject the entire move.

The precise mechanics of the sampler are not shown here; some additional technical issues are discussed in Appendix 7.2.

3.2. Technical considerations

Almost as important as how the method works is when it is sound to use (or not!). Since the package is intended to be used primarily by practitioners, one of the aims of this paper is to clarify what types questions **BPEC** can potentially answer as well as what underlying assumptions are necessary and implicit.

Bayesian Phylogeographic and Ecological Clustering assumes that non-recombinant (typically mtDNA) data are available from a set of geographical locations (in the form of longitude/latitude). The haplotype tree model takes a relaxed parsimony approach, which, in cases of deep divergence, excessive homoplasy or too many unknown mutations, will be unreliable. **BPEC** is programmed to produce appropriate error messages to inform the user in such cases, but will not be foolproof. A potential workaround may be to use **Gblocks** (Talavera and Castresana 2007), **Noisy** (Dress et al. 2008), or **Aliscore** (Misof and Misof 2009) to remove problematic (poorly aligned/divergent) nucleotide sites before inputting the sequences into **BPEC**.

The geographical model assumes a constant population size and migration rate; if such assumptions are clearly violated, or if differences in population sizes and migration rates are indeed quantities of interest, **BPEC** is not appropriate to use. Also, the clustering and migration model does not explicitly take into account geographical distance between clusters. It simply separates observations in distinct geographical clusters. Therefore, it is possible for a migration to result in two distant clusters.

Notice that we assume a uniform prior over the number of migrations K . In general, K migrations can lead to up to $K + 1$ clusters; often, however, some of these may be empty, resulting in fewer ‘effective’ migrations. The uniform prior applies to the total number of migrations rather than the number of effective ones, whereas the posterior distribution over the number of migrations actually refers to effective migrations. This somewhat convoluted approach is preferred because enumerating scenarios of different effective migrations is computationally cumbersome.

As discussed earlier, an important consideration when using **BPEC** for ancestral inference is the distribution of haplotype observations within each location. Since ancestral location probabilities are determined through the proportion of ancestral haplotypes, locations with e.g. a single haplotype which happens to be ancestral will always result in high probability of being ancestral. Consequently, ancestral location probabilities are generally more reliable the more observations are available per location.

One of the limitations of Markov chain Monte Carlo methods is that the samplers require a large number of iterations to satisfy convergence diagnostics. The convergence diagnostics in **BPEC** are split into two pieces: convergence of the clustering and convergence of the root haplotype. If either of these two pieces has not converged, the sampler will return an error to that effect. Ideally, both pieces should satisfy the convergence diagnostics; however, it is sometimes the case (especially when dealing with a large number of clusters) that, for any reasonable number of MCMC iterations, the diagnostics fail. In these cases, inferences should be taken with caution.

It also frequently occurs that uncertainty about the root haplotype is high, with several different haplotypes carrying significant posterior mass. This is to be expected, especially with datasets that show divergence, lots of missing intermediate haplotypes or have no ‘clear’ root pattern. However, ancestral location inferences often show lower uncertainty despite an unknown precise root haplotype. As long as no convergence errors are reported, this is not a convergence issue but merely reflects uncertainty in the conclusions.

BPEC cannot deal with unknown nucleotides and will ignore any nucleotide sites at which one of sequences has an unknown nucleotide (denoted as ‘?’). This means that unknown nucleotides result in information loss. On the other hand, **BPEC** will treat true alignment

gaps '-' as a 5th character such that a deletion/insertion is treated as a type of mutation. Care should be taken in the interpretation of the output when lots of missing nucleotides are present, since this could lead to significant loss of resolution (Joly *et al.* 2007).

Finally, although not explicitly modelled with **BPEC**, the presence or absence of correlation of geography with genetic pattern observed can lead to inferences about the phylogeographical component of population evolutionary history like the potential of gene flow across geographic areas (population splitting and dispersal), hybridization between species (secondary gene flow by population re-joining), and aspects of demographic dynamics of the populations under study (lineage sorting by frequency shifts of haplotypes).

4. User interface

4.1. Inputs

BPEC takes two main inputs: the set of mtDNA sequences (in NEXUS format) and the set of coordinates and haplotypes observed in each location. Sequences need not be collapsed onto haplotypes, but labelling of sequences in the NEXUS file and the locations file must be consistent. In order to load these two variables into R from two files called **Haplotypes.nex** and **CoordsLocsFile.txt** (for example), the following commands can be used.

The sequences can be loaded using the `read.nexus.data` command of package **ape** (included in **BPEC**).

```
R> library(BPEC)
R> RawSeqs = read.nexus.data('Haplotypes.nex')
```

The file containing the list of coordinates and covariates needs to have, in each line, a longitude, latitude, environmental/phenotypic covariate values (if available), plus a set of numbers corresponding to the haplotypes/sequences with these attributes. For example, for two locations with 5 observations in total from 3 haplotypes, with no additional covariates, the file might read

```
40.3 45.2    1    2    2
45.3 50.1    2    3
```

All haplotypes/sequences found in a location can be entered in one line, or only one per row, such that we could also have used

```
40.3 45.2    1
40.3 45.2    2    2
45.3 50.1    2    3
```

or any such combination.

When additional environmental or phenotypic covariates are available, these can also be entered as a column right after the longitude and latitude, such as

```
40.3 45.2 18.1    1
40.3 45.2 22.5    2    2
45.3 50.1 25.0    2    3
```

where 18.1, 22.5, 25.0 are, for example, temperatures. Environmental covariates can be extracted, for example, from publicly available databases such as bioclim by means of the R-package **raster**.

In order to load this file containing the coordinates, covariates and observed haplotypes/sequences of each location, use the `read.table` command below.

```
R> CoordsLocs = read.table('CoordsLocsFile.txt',header=FALSE,fill=TRUE,
+                          col.names=1:max(count.fields('CoordsLocsFile.txt')))
```

The `fill=TRUE` and `col.names=1:max(count.fields('CoordsLocsFile.txt'))` are necessary because the list of observations in each location may be of unequal length.

Names for the covariates at each location can optionally be provided through

```
R> colnames(CoordsLocs)[1:8] = c('lat','long','cov1','cov2',
+                               'cov3','cov4','cov5','cov6')
```

These coordinate names will later appear in the output plots to aid interpretation.

4.2. Main MCMC command and options

Once the `RawSeqs` and `CoordsLocs` variables have been loaded, the Markov chain Monte Carlo sampler can be run through the command

```
R> MCMCout = BPEC.MCMC(RawSeqs,CoordsLocs,MaxMig,iter,ds,PostSamples,dims)
```

The options here are chosen as follows.

- **MaxMig**: the maximum number of migrations to be considered. In terms of inference, the higher **MaxMig**, the better the results, since more models are considered. However, that comes at a computational cost. We recommend using a value of 6 (corresponding to 7 clusters), and if the inference shows significant posterior probability on 7 clusters, increase **MaxMig** and re-run. Similarly, if e.g. a value of 5 is used and convergence diagnostics are not satisfied, but posterior mass seems to be minimal around 4/5 migrations, then one can reduce **MaxMig** to 4 (which will reduce complexity) and re-run.
- **iter**: the number of MCMC iterations to run the sampler for. By default, two chains will be run from different starting values. The value of **iter** is important, as it will determine how long the chains will run for and whether convergence (both in terms of the root haplotype as well as the clustering) diagnostics will be satisfied. A value of 100,000 is usually reasonable to start with; if convergence diagnostics are not satisfied, or if the post-processing plots look inconsistent, increase **iter** by a factor of 10 (and so on).

- **ds**: the parsimony relaxation parameter d_s . We recommend starting with $d_s = 0$ and increasing once reasonable values of **iter** and **MaxMig** have been established. Note that increasing d_s past an (unknown) value d_{max} , which depends on the individual dataset, has no effect on the inference.
- **PostSamples**: the number of posterior samples (per chain) to be saved for posterior summary statistics. We recommend using a value around 1,000. The higher the better for inference, but this comes at a memory storage cost.
- **dims**: the number of covariates (including longitude and latitude) available. If only geographical data are used (and no environmental or phenotypic information), **dims**=2. Otherwise increase as appropriate.

4.3. Outputs

The **BPEC.MCMC** command outputs a large list that can be accessed via e.g. **MCMCout\$SeqR**, similarly **MCMCout\$CoordsLocsR** etc.

- Variables that arise directly from the data
 - **SeqR**: The output DNA sequences of distinct haplotypes (both sampled and missing which were inferred), showing only effective nucleotides (if two different nucleotide sites are variable in exactly the same haplotypes, then they effectively provide information of a single site).
 - **CoordsLocsR**: A matrix where each row has the coordinates of each location (lat/long), any environmental covariates, plus the haplotypes found at each location. All rows will have the same length, so sampling locations with fewer sampled sequences will be filled with NAs.
 - **CoordsDimsR**: the dimension of the input (2 for geographical, +1 for every additional environmental/phenotypic covariate).
 - **LocNoR**: the number of distinct sampling locations.
 - **NoSamplesR**: a vector of the number of times each haplotype was observed.
 - **SeqCountR**: the number of input sequences.
 - **countR**: the total number of haplotypes (observed and unobserved) in the tree defined by Ω .
 - **SeqLengthR**: the effective length of the input sequences, given by the number of variable nucleotide sites which are informative.
 - **SeqsFileR**: a vector of the numerical labels of each haplotype.
 - **SeqLabelsR**: the correspondence vector each of the processed observations to the original haplotype labels.
- Variables that correspond to MCMC output of the geographical pieces of the model:
 - **PostMeansR**: posterior means of the cluster centres.
 - **PostCovsR**: posterior means of the cluster covariances.

- **SampleMeansR**: a set of **PostSamples** posterior samples of the cluster centres.
- **SampleCovsR**: a set of **PostSamples** posterior samples of the cluster covariances.
- Variables that correspond to MCMC output of the tree model:
 - **cladoR**: the adjacency matrix for the Maximum a Posteriori tree in vectorised format. For two haplotypes i, j , the (i, j) th entry of the matrix is 1 if the haplotypes are connected in the network and 0 otherwise.
 - **TreeEdges**: contains the same information as **cladoR**, but in a different format. The set of edges (from and to haplotypes) of the Maximum A Posteriori haplotype tree are represented as a list of from/to vectors which could be used in another program if needed (e.g., **igraph**).
 - **EdgeTotalProbR**: Posterior probabilities of each edge being present in the tree, so that any edge which is not part of a loop will have posterior probability 1.
 - **MigProbsR**: a vector of the posterior probabilities of $\{0 \dots \text{MaxMig}\}$ migrations.
 - **RootProbsR**: a vector of the posterior probabilities that each haplotype is the root of the tree.
 - **RootLocProbsR**: a vector of the posterior probabilities of each sampling location being the most ancestral location. Since sampling locations are collapsed to unique ones, if several rows in the file **CoordsLocsFile.txt** correspond to the same geographical location, the first of these will carry the total posterior probability for the location, with the remaining having 0.
 - **ClusterProbsR**: for each haplotype, posterior probabilities that it belongs to each cluster.
 - **levelsR**: Starting from the root (level 0) all the way to the tips, the discrete depth for the Maximum A Posteriori tree.
- MCMC tuning:
 - **MCMCparamsR**: various tuning parameters used in the MCMC sampler, this is only important for development.
 - **MCChainMeansR**: Posterior means for each dimension of the centre of each cluster for each of the two MCMC chains.
 - **CodaInput**: Posterior samples from the two MCMC chains for the cluster means, cluster covariance entries, as well as the root haplotype. Note that, since the number of clusters varies from iteration to iteration, some samples are simply draws from the prior (corresponding to empty clusters). This variable can be loaded directly into the coda package for convergence analysis.

4.4. Visualizations and Post-processing

As described in the previous section, the Markov chain Monte Carlo sampler returns many different types of outputs. In order to obtain a summarised picture of the inference, a number of visualizations are available through **BPEC** to aid interpretation. The commands are illustrated on a brown frog dataset which can be loaded through


```
R> data("MacrocnemisRawSeqs")
R> data("MacrocnemisCoordsLocs")
R> RawSeqs = MacrocnemisRawSeqs
R> CoordsLocs = MacrocnemisCoordsLocs
```

which contains 40 sequences together with their corresponding longitude/latitude, along with 6 environmental covariates. Other datasets that are available in **BPEC** can be found using `data(package='BPEC')`. The analysis is then carried out using

```
R> set.seed(108)
R> MCMCout = BPEC.MCMC(RawSeqs,CoordsLocs,MaxMig=3,iter=1000000,
+                      ds=3,PostSamples=1000,dims=8)
```

```
Starting BPEC...
Inferring possible missing sequences....
Counting loops in the network...
```

The program found no loops that need to be resolved in the network

```
Number of iterations is 1000000
Number of saved iterations 1000
Sample size is 40
Effective sequence length is 8
Total number of haplotypes (including missing) 10
Dimension is 8
Parsimony relaxation is 3
Maximum number of migrations is 3
```

```
Starting the MCMC sampler (burn-in ends at 90% and acceptance rate re-started):
Chain 1: |=====|100% (accepted samples    2763 time   24 minutes)
Chain 2: |=====|100% (accepted samples    2823 time   49 minutes)
```

```
The most likely root node is 2
The most likely ancestral locations are 38,34,4
```

and post-processed using the commands described in this section.

Geographical contour plot

The command `BPEC.ContourPlot` provides a colour-coded contour plot of the geographical clusters superimposed onto a map (provided accurate longitude and latitude coordinates have been provided). In order to convey not only posterior means but also uncertainty, a set of posterior draws of these contours are plotted using transparency, so that the user can assess the stability of the inference. A ‘messy’ looking plot either implies poor MCMC convergence or high uncertainty in terms of the clustering.

The sampling locations are also shown on this contour plot, with the top three sampling locations in terms of their probability of being ancestral shown in larger triangles. An example

of a `BPEC.ContourPlot` is shown in Figure 6 using the brown frog dataset described in Section 5. The colours can be changed through the optional variable `colorcode` (with default value `(7,5,6,3,2,8,4,9,10)`) which controls the colour of the first, second, third cluster etc; if not specified, the default colour scheme is used.

```
R> BPEC.ContourPlot(MCMCout,CoordsLocs,GoogleEarth=0,colorcode=c(7,5,6,3,2))
```

Instead of using the in-built R maps, the contour plot can also be exported into GoogleEarth format using the option `GoogleEarth=1`. This will produce a set of `kml` extension files which can be loaded directly into GoogleEarth.

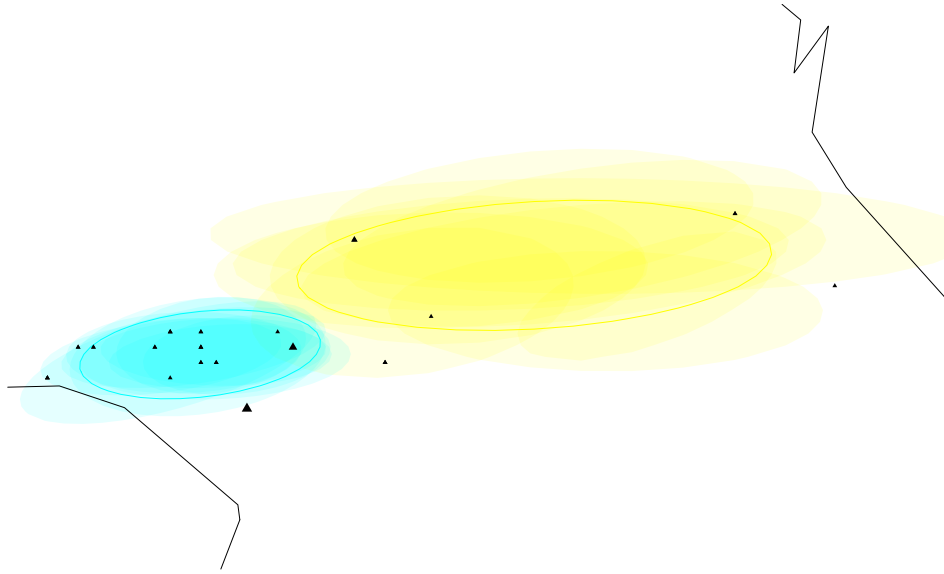


Figure 6: An example of the contour plot for the brown frog dataset using `BPEC.ContourPlot`. The transparent geographical clusters show posterior draws of the center within 50% concentration contours of each cluster. Solid ellipses represent posterior means. Larger triangles represent most likely ancestral locations. The black jagged lines show the outline of the geographical map of the area.

Environmental and/or phenotypic covariates plot

In cases where environmental or phenotypic covariates have also been used, posterior draws of the distribution of the covariates within clusters are available through `SampleMeansR` and `SampleCovsR`. These can be summarized through posterior medians and 5/95% credible regions, colour-coded using the same coding as the contour plot. To aid plotting and interpretation, the covariate names of each of the columns of `CoordsLocs` are used. The first two (corresponding to longitude and latitude) are automatically ignored in this function.

```
R> par(mfrow=c(2,3))
R> BPEC.CovariatesPlot(colnames(CoordsLocs),MCMCout,colorcode=c(7,5,6,3,2))
```

An example of the plot produced in the case of the brown frog dataset is shown in Figure 7.

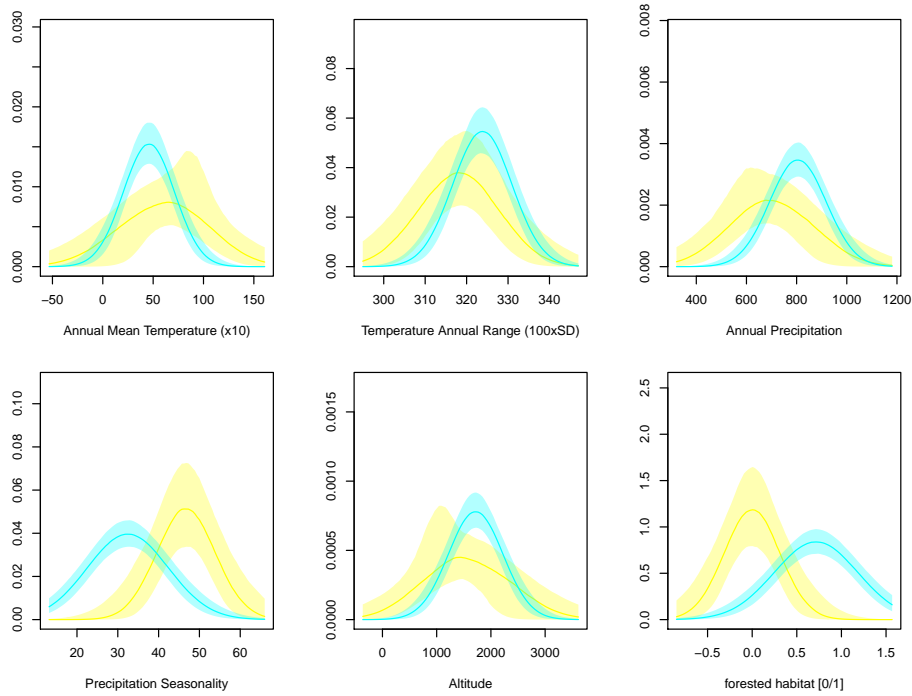


Figure 7: Plot of the distribution of the covariates for each cluster for the brown frog dataset using `BPEC.CovariatesPlot`. Shaded regions correspond to 5% and 95% pointwise credibility bands of each cluster, with solid lines showing the pointwise median.

Clustered tree plot

To visualize the Maximum A Posteriori haplotype tree, the command `BPEC.Tree` plots the haplotype tree most supported by the data. The size of each node in the tree represents the number of times each haplotype was observed, black dots corresponding to missing intermediate haplotypes. The thickness of each edge represents the posterior probability that each mutation occurred (thin edges corresponding to mutations with high uncertainty). Observed haplotypes are colour-coded according to their posterior probability of belonging to each cluster. As long as the same `colorcode` variable is used, the cluster colours correspond to the ones used in the geographical and covariate contour plots.

```
R> BPEC.Tree = BPEC.TreePlot(MCMCout,colorcode=c(7,5,6,3,2))
```

The corresponding plot for the brown frog dataset is shown in Figure 8.

Tree plot on geographical map

The tree plot can also be partially visualised geographically through the `BPEC.GeoTree` command which superimposes the haplotype tree onto a map through a file that can be loaded into Google Earth. The function uses the `igraph` package (Csardi and Nepusz 2006) as well as `phytools` (Revell 2012) and (Valiente 2010) in order to convert the network into newick format and then visualize it as an interactive tree. Finally, to overlay the tree onto the map, the library `R2G2` is used (Arrigo et al. 2012; Arrigo 2013). Since haplotypes can be observed

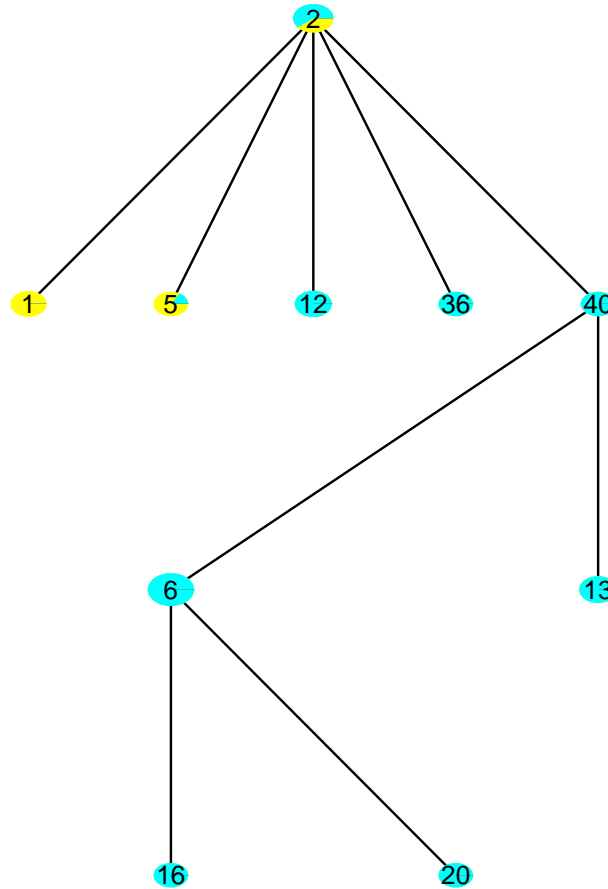


Figure 8: Clustered tree plot of the brown frog dataset using `BPEC.TreePlot`. Colour corresponds to cluster membership probability and size of node to the number of individuals sampled with each sequence. Edges represent single effective mutations and black dots represent unobserved intermediate haplotypes. In this case all edges have effectively no posterior uncertainty under the model, so they all appear with equal thickness.

in multiple locations, clicking on particular nodes of the tree shows the locations where each copy of the haplotype was found. However, when multiple haplotypes were found in a single location, only one will be displayed, so the `BPEC.GeoTree` may not tell the whole story. Also note that only existing tip haplotypes are possible to identify on the map.

```
R> BPEC.Geo = BPEC.GeoTree(MCMCout,CoordsLocs,file="GoogleEarthTree.kml")
```

An example is shown in Figure 9. Tip haplotypes are connected to a tree by a single branch, internal node haplotypes have three or more connections, whereas branch haplotypes exactly two connections.

5. Analysis of brownfrog data

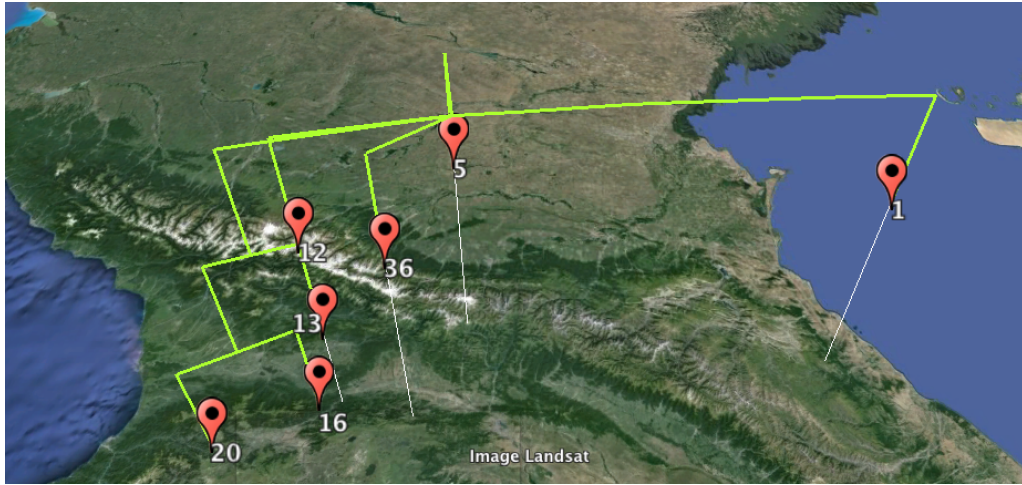


Figure 9: A projection of the haplotype tree in Figure 8 on the corresponding geographical map using Google Earth.

We used 40 mitochondrial cytochrome b sequences of Near Eastern brown frogs - taxon *Rana macrocnemis* (Boulenger, 1885) - accessible through GenBank (Tarkhnishvili et al. 2001; Veith et al. 2003b,a) to demonstrate a combined phylogeographic and ecological analysis with **BPEC**. The evolutionary history of the brown frogs, as part of a thorough phylogenetic (Veith et al. 2003a) and a phylogeographic Nested Clade analysis (Veith et al. 2003b) has been described by scenarios of range expansion and fragmentation triggered by Pleistocene glaciation cycles and associated dramatic climatic oscillations over at least 2 Mya years, most intensified during the last 600,000 years. Within the whole distribution of this polytypic species, we focus on two forms that coexist in a narrow contact zone in the Minor Caucasus: the nominotypic *R. macrocnemis macrocnemis* (Boulenger, 1885) living on the forested slopes of the Trialeti ridge northwest and on montane meadows on both sides of the Great Caucasus, and *R. macrocnemis camerani* (Boulenger, 1885) in southern Georgia on the Javakheti plateau (Tarkhnishvili et al. 2001).

BPEC was applied to investigate the concordance of phylogeographic population clusters with habitat type or landscape structure which is consistent with the hypothesis of ecological speciation. Ecological speciation is the evolution of barriers to gene flow between populations resulting from ecologically-based divergent selection between different environments (Nosil 2012). Therefore, we included predictive environmental and climate covariates (topographic and land cover conditions, and annual trend patterns of temperature, precipitation and seasonality) to determine the interplay of environmental gradients and divergent selection / adaptation regimes. Grid-based attribute values of a set of predictor variables associated with each cell position of the map layers were subsequently extracted at the point locations of the geo-referenced mtDNA haplotypes from six raster grids by means of the `extract` function of the **raster** package (Hijmans et al. 2016): four bioclimatic variables from the www.worldclim.org database (Annual Mean Temperature (degrees Celsius x 10), Temperature Annual Range (100 × standard deviation of monthly mean temperature), Annual Precipitation (in mm), Precipitation Seasonality (Coefficient of Variation (CV)), altitude in meters as a proxy for a digital elevation model (DEM) and the land cover map (GLC2000) from worldgrids.org. We re-classified the total information of the land cover map into two classes of forested and non-

forested areas to introduce a simplistic landscape dependent habitat variable (COV). These six variables altogether describe climatic, topographic, and land cover conditions that were suggested as the key predictors for the differential occurrence of both lineages of Caucasian brown frogs.

The hypotheses of interest were whether differences in the corresponding geographical clusters are associated with a transition in environmental factors such as a transition in the landscape (open=non-forest vs. forested areas; COV), amount of rainfall and average altitude (a measure which is widely used as a surrogate for environmental gradients).

The dimensionality of the data was $p = 8$ (**CoordsDimsR**), for geographical dimensions longitude and latitude plus the six additional environmental covariates. **BPEC** detected 10 distinct haplotypes with effective length 8 (corresponding to the number of informative variable nucleotide sites). The haplotypes result from a reduction of the full length (504 bp) of the original sequences to the number of parsimony informative sites only and are displayed in the MAP haplotype tree shown in Figure 8. We ran the **BPEC** analysis for 1,000,000 iterations (**iter**) each, taking the maximum parsimony level option at minimum, **ds** = 0. Convergence diagnostics of the maximum a posteriori (MAP) clusterings and root were not violated (i.e., no convergence error message was reported).

The posterior mass for the number of clusters strongly concentrates around 2 (as indicated by **MigProbsR**), with the posterior probability of 2 clusters being greater than 0.99. These are shown in Figure 6. The clusters refer to two population groups that cannot be simply designated as the two evolutionary lineages *R. macrocnemis macrocnemis* and *R. macrocnemis camerani*. The phylogenetically older ancestral lineage (in yellow) as indicated by the root population of Central Daghestan, can be taxonomically called the nominotypic *R. macrocnemis macrocnemis* lineage. The turquoise cluster comprises a genetically homogeneous population group that includes populations from the humid and forested mountain part of the *macrocnemis* range, and the “*camerani*-like” populations from the drier area of the southern treeless mountain steppe habitats of the Javakheti plateau. The contour ellipses overlap in the heart of the geographic transition zone south of the Minor Caucasus. For simplicity we denote the two clusters “ancestral *macrocnemis*-like” (yellow) and “populations of the contact zone” (turquoise), respectively.

Identifying ancestral locations revealed the following locations with top posterior probability:

- Most likely ancestral location with posterior probability 24% were the geositions of observations (38,39,40) (Paravani lake, treeless mountain steppe, 2100m, Javakheti plateau, *camerani* population).
- With posterior probability 12% were the geositions of observations (34,35,36,37) (Tsalka, sample locality of *camerani*, treeless mountain steppe, close to the southern slopes of the Trialeti Ridge, mainly *camerani*-like morphotypes up to 74% in the population). This population is also genetically comprised of a haplotype with two colours, indicating its posterior probability of belonging to each of the corresponding clusters (mainly the turquoise “forest” cluster with a smaller probability of the yellow “non-forest” cluster).
- Location of observations (4,5,6) (Cross Mountain Pass, sample locality of *macrocnemis*, alpine habitat, 2000-2500m, Great Caucasus), posterior probability about 10%. Cross Pass represents two distinct classes of haplotypes that correspond either to the “forest”

cluster (turquoise, haplotype 6 with higher frequency in the site) and the “non-forest” cluster (yellow).

Thus, ancestral sites lie either in the drier uplands of the Javakheti plateau (Paravani, a typical *camerani* habitat) and south of the Trialeti Ridge (Tsalka), or on the other extreme in alpine meadows of the Great Caucasus (Cross Pass, a well-known locality for *macrocnemis*). The main ancestral site for the *camerani* expansion lies more southern in the treeless Javakheti plateau (Paravani).

The mixed population Tsalka is located on the southern treeless foothills of the Trialeti Ridge, which has a more humid climate with forested landscape spreading northwards. The haplotypes of the morphologically mixed population Tsalka mainly correspond to the “forest” cluster. This ancestral site can be interpreted as the link, which mediates the genetical differentiation and ecological divergence in the closer transition zone marked by the overlap of the contour ellipses. Interestingly, the overlapping centre between the two clusters of haplotype diversity coincides well with the gradient in population assignments over the contact zone as derived from microsatellite genotype frequencies and calculated by means of the **GENELAND** R-package. The extent of the geographic area within populations share common coalescence as measured by maternally transferred mtDNA is however broader and shifted to the east than is the case when detected by means of recombinant microsatellite markers (Hille et al. 2015).

The root location of all populations of the *macrocnemis* lineage is found most distant to the East in Central Daghestan, giving rise to the differentiation patterns of the two divergent population clusters. All cis- and trans-Caucasian sampling locations covered by the yellow contour ellipse and crossing the Great Caucasus can be supposed to represent the phylogenetically oldest population cluster of the eastern lineage of Near Eastern brown frogs, lineage descendants out of the early Pleistocene Transcaucasian / Pontic refugium..

The clusters of the bioclimatic variables (annual mean temperature, annual range of temperature, annual precipitation, precipitation seasonality) and altitude, shown in Figure 7, are separated mainly due to the difference in the means of these environmental conditions within each cluster rather than their variances. Differences in means are especially apparent for the annual mean temperature ($> 5^{\circ}\text{C}$ for *macrocnemis*, around 5°C for populations of the contact zone), annual range of temperature (high amplitude of variation, typical for mountain climates: $\text{CV} < 320\%$ for *macrocnemis*, $> 320\%$ for populations of the contact zone), annual precipitation (higher for populations of the contact zone, nearly 800mm), annual distribution of precipitation (much higher in the ancestral *macrocnemis* population, $\text{CV} > 45\%$ which results in longer periods without rain and if it rains, higher volumes of rain fall). Altitude is rather similar around 1500-1800m (lower altitude for *macrocnemis*). Finally, the landscape dependent variable “open vs. forested habitat” is clearly different for the two population groups, the populations of the contact zone show around 75% forested habitats. These findings are in agreement with the hypothesis that the two clusters are not only geographically and genetically separated, but they are also followed by clear environmental differences.

6. Discussion

We have described **BPEC**, a user-friendly implementation of the phylogeographic and ecological clustering methods described in Manolopoulou and Emerson (2012); Manolopoulou et al.

(2011). We have introduced several visualization and post-processing tools in order to aid data analysis and interpretation, along with details of the significance of different types of output. **BPEC** will continue to be improved. The main focus of the extensions will revolve around speeding up the convergence of the sampler and improving the approximation stemming from the auxiliary tree parameter. We also intend to work on export functions of the mapping results in spatial object classes, for example provided by the **sp** package (Pebesma and Bivand 2005).

In terms of extensions to the actual model, more generic evolutionary models for the haplotype trees will be gradually introduced. Similarly, explicitly modelling the migration process as a spatial transition will allow additional information from the spatial distribution to inform the tree and vice versa.

Finally, we are investigating whether we can extend the applicability of **BPEC** to the interface of species and closely related species groups, geographical subspecies, and vicariant sister species. **BPEC** should actually be applicable to the examination of genealogy of closely related populations under the evolutionary scenario of successive population splitting and dispersion events (the classical allopatric, allo-parapatric and peripatric modes (I, II) of geographic speciation (Wiley and Lieberman 2011)), where lineage sorting occurs in ancestral populations that have yet to diverge.

Acknowledgements

AH thanks D. Tarkhnishvili for his expert comments on the brown frogs. N. Arrigo, T. Nepusz, L. Revell and G. Valiente quickly answered questions on R functions they published, many thanks to them all.

References

- Arrigo N (2013). **R2G2: Converting R CRAN outputs into Google Earth**. R package version 1.0-2, URL <https://CRAN.R-project.org/package=R2G2>.
- Arrigo N, Albert LP, Mickelson PG, Barker MS (2012). “Quantitative visualization of biological data in Google Earth using R2G2, an R CRAN package.” **Molecular ecology resources**, **12**(6), 1177–1179.
- Atteson K (1999). “The Performance of Neighbor-Joining Methods of Phylogenetic Reconstruction.” **Algorithmica**, **25**, 251–278.
- Avice JC, Arnold J, Ball RM, Bermingham E, Lamb T, Neigel JE, Reeb CA, Saunders NC (1987). “Intraspecific phylogeography: the mitochondrial DNA bridge between population genetics and systematics.” **Annual review of ecology and systematics**, pp. 489–522.
- Beaumont M (2003). “Estimation of Population Growth or Decline in Genetically Monitored Populations.” **Genetics**, **164**, 1139–1160.
- Beaumont MA, Nielsen R, Robert C, Hey J, Gaggiotti O, Knowles L, Estoup A, Panchal M, Corander J, Hickerson M, et al. (2010). “In defence of model-based inference in phylogeography.” **Molecular Ecology**, **19**(3), 436–446.

- Bielejec F, Rambaut A, Suchard MA, Lemey P (2011). “SPREAD: spatial phylogenetic reconstruction of evolutionary dynamics.” **Bioinformatics**, **27**(20), 2910–2912.
- Bloomquist EW, Lemey P, Suchard MA (2010). “Three roads diverged? Routes to phylogeographic inference.” **Trends in ecology & evolution**, **25**(11), 626–632.
- Cornuet JM, Pudlo P, Veyssier J, Dehne-Garcia A, Gautier M, Leblois R, Marin JM, Estoup A (2014). “DIYABC v2. 0: a software to make approximate Bayesian computation inferences about population history using single nucleotide polymorphism, DNA sequence and microsatellite data.” **Bioinformatics**, **30**(8), 1187–1189.
- Csardi G, Nepusz T (2006). “The igraph software package for complex network research.” **InterJournal, Complex Systems**, 1695. URL <http://igraph.org>.
- De Iorio M, Griffiths R (2004a). “Importance sampling on coalescent histories. I.” **Advances in Applied Probability**, **36**, 417–433.
- De Iorio M, Griffiths R (2004b). “Importance sampling on coalescent histories. II: Subdivided population models.” **Advances in Applied Probability**, **36**, 434–454.
- Desper R, Gascuel O (2002). “Fast and Accurate Phylogeny Reconstruction Algorithms Based on the Minimum-Evolution Principle.” In **WABI '02: Proceedings of the Second International Workshop on Algorithms in Bioinformatics**, pp. 357–374. Springer-Verlag.
- Dress AW, Flamm C, Fritzsche G, Grünewald S, Kruspe M, Prohaska SJ, Stadler PF (2008). “Noisy: identification of problematic columns in multiple sequence alignments.” **Algorithms for Molecular Biology**, **3**(1), 1.
- Drummond AJ, Suchard MA, Xie D, Rambaut A (2012). “Bayesian phylogenetics with BEAUti and the BEAST 1.7.” **Molecular biology and evolution**, **29**(8), 1969–1973.
- Dyer RJ, Nason JD (2004). “Population graphs: the graph theoretic shape of genetic structure.” **Molecular Ecology**, **13**(7), 1713–1727.
- Ethier SN, Griffiths RC (1987). “The Infinitely-Many-Sites Model as a Measure-Valued Diffusion.” **The Annals of Probability**, **15**, 515–545.
- Felsenstein J (1983). “Statistical Inference of phylogenies.” **Journal Of The Royal Statistical Society Series A**, **146**, 246–272.
- Gascuel O, Steel M (2006). “Neighbor-Joining Revealed.” **Molecular Biology and Evolution**, **23**, 1997–2000.
- Guillot G, Mortier F, Estoup A (2005). “GENELAND: a computer package for landscape genetics.” **Molecular Ecology Notes**, **5**(3), 712–715.
- Hein J, Schierup M, Wiuf C (2004). **Gene genealogies, variation and evolution: a primer in coalescent theory**. Oxford university press.
- Hijmans RJ, Phillips S, Leathwick J, Elith J (2016). **dismo: Species Distribution Modeling**. R package version 1.0-15, URL <https://CRAN.R-project.org/package=dismo>.

- Hille A, Manolopoulou I, Tarkhnisvili D (2015). “Detecting landscape-dependent selection with Bayesian phylogeographic and ecological clustering: comparison of recombinant microsatellite and mtDNA haplotype data.”
- Huelsenbeck J, Ronquist F (2001). “MrBayes: Bayesian inference on phylogenetic trees.” **Bioinformatics**, **17**, 754–755.
- Joly S, Stevens MI, van Vuuren BJ (2007). “Haplotype networks can be misleading in the presence of missing data.” **Systematic Biology**, **56**(5), 857–862.
- Jombart T, Devillard S, Balloux F (2010). “Discriminant analysis of principal components: a new method for the analysis of genetically structured populations.” **BMC genetics**, **11**(1), 94.
- Kingman J (1982). “The coalescent.” **Stochastic Processes and their Application**, **13**(3), 235–248.
- Knowles LL (2009). “Statistical phylogeography.” **Annual Review of Ecology, Evolution, and Systematics**, **40**, 593–612.
- Knowles LL, Maddison WP (2002). “Statistical phylogeography.” **Molecular Ecology**, **11**(12), 2623–2635.
- Knuth D (1998). “Sorting and searching.” In **The art of Computer programming**, volume 3. Addison-Wesley.
- Leblois R, Pudlo P, Néron J, Bertaux F, Beeravolu CR, Vitalis R, Rousset F (2014). “Maximum likelihood inference of population size contractions from microsatellite data.” **Molecular biology and evolution**, pp. 2805–2823.
- Lemey P, Rambaut A, Drummond AJ, Suchard MA (2009). “Bayesian phylogeography finds its roots.” **PLoS computational biology**, **5**(9), e1000520.
- Manolopoulou I, Emerson BC (2012). “Phylogeographic Ancestral Inference Using the Coalescent Model on Haplotype Trees.” **Journal of Computational Biology**, **19**(6), 745–755.
- Manolopoulou I, Legarreta L, Emerson BC, Brooks S, Tavaré S (2011). “A Bayesian approach to phylogeographic clustering.” **Interface focus**, p. rsfs20110054.
- Misof B, Misof K (2009). “A Monte Carlo approach successfully identifies randomness in multiple sequence alignments: a more objective means of data exclusion.” **Systematic Biology**, **58**(1), 21–34.
- Nosil P (2012). **Ecological speciation**. Oxford University Press.
- Panchal M, Beaumont MA (2007). “The automation and evaluation of nested clade phylogeographic analysis.” **Evolution**, **61**(6), 1466–1480.
- Papastamoulis P, Iliopoulos G (2010). “An artificial allocations based solution to the label switching problem in Bayesian analysis of mixtures of distributions.” **Journal of Computational and Graphical Statistics**, **19**(2).

- Pebesma EJ, Bivand RS (2005). "Classes and methods for spatial data in R." **R news**, **5**(2), 9–13.
- Pritchard JK, Stephens M, Donnelly P (2000). "Inference of population structure using multilocus genotype data." **Genetics**, **155**(2), 945–959.
- R Core Team (2015). **R: A Language and Environment for Statistical Computing**. R Foundation for Statistical Computing, Vienna, Austria. URL <https://www.R-project.org/>.
- Ranjard L, Welch D, Paturel M, Guindon S (2014). "Modelling Competition and Dispersal in a Statistical Phylogeographic Framework." **Systematic Biology**, **63**(5), 743–752. ISSN 1063-5157, 1076-836X.
- Revell LJ (2012). "phytools: An R package for phylogenetic comparative biology (and other things)." **Methods in Ecology and Evolution**, **3**, 217–223.
- Ronquist F, Sanmartín I (2011). "Phylogenetic methods in biogeography." **Annual Review of Ecology, Evolution, and Systematics**, **42**(1), 441.
- Rzhetsky A, Nei M (1993). "Theoretical foundation of the minimum-evolution method of phylogenetic inference." **Molecular Biology and Evolution**, **10**, 1073–1095.
- Sanmartín I, Anderson CL, Alarcon M, Ronquist F, Aldasoro JJ (2010). "Bayesian island biogeography in a continental setting: the Rand Flora case." **Biology letters**, pp. 703–707.
- Stephens M (2000a). "Bayesian Analysis of Mixture Models with an Unknown Number of Components- An Alternative to Reversible Jump Methods." **The Annals of Statistics**, **28**, 40–74.
- Stephens M (2000b). "Dealing with label-switching in mixture models." **Journal of the Royal Statistical Society. Series B (Methodological)**, **62**, 795–809.
- Talavera G, Castresana J (2007). "Improvement of phylogenies after removing divergent and ambiguously aligned blocks from protein sequence alignments." **Systematic biology**, **56**(4), 564–577.
- Tarkhnishvili D, Hille A, Böhme W (2001). "Humid forest refugia, speciation and secondary introgression between evolutionary lineages: differentiation in a Near Eastern brown frog, *Rana macrocnemis*." **Biological Journal of the Linnean Society**, **74**(2), 141–156.
- Templeton A (1998). "Nested clade analysis of phylogeographic data: testing hypotheses about gene flow and population history." **Molecular Ecology**, **7**, 381–397.
- Templeton AR (2004). "Statistical phylogeography: methods of evaluating and minimizing inference errors." **Molecular Ecology**, **13**(4), 789–809.
- Valiente G (2010). **Combinatorial pattern matching algorithms in computational biology using Perl and R**. CRC Press.
- Veith M, Kosuch J, Vences M (2003a). "Climatic oscillations triggered post-Messinian speciation of Western Palearctic brown frogs (Amphibia, Ranidae)." **Molecular phylogenetics and evolution**, **26**(2), 310–327.

- Veith M, Schmittler J, Kosuch J, Baran I, Seitz A (2003b). “Palaeoclimatic changes explain Anatolian mountain frog evolution: a test for alternating vicariance and dispersal events.” **Molecular Ecology**, **12**(1), 185–199.
- Wakeley J (2013). “Coalescent theory has many new branches.” **Theoretical population biology**, **87**, 1.
- Wiley EO, Lieberman BS (2011). **Phylogenetics: theory and practice of phylogenetic systematics**. 2nd edition. John Wiley & Sons.

7. Appendix

7.1. Temporal orderings

Suppose the haplotype tree is given by the top tree of Figure 10 (Manolopoulou and Emerson 2012). For ease of exposition, the numbers on the nodes here represent the sample sizes of each haplotype rather than the label of each haplotype.

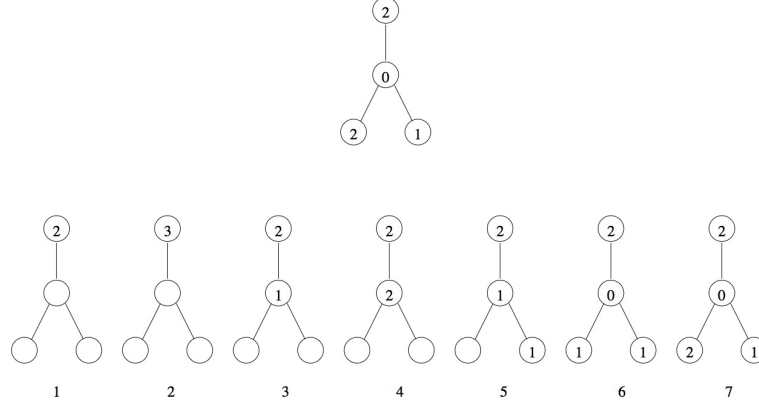


Figure 10: Top panel: In this tree the oldest haplotype of the sample (the top haplotype) is observed twice in the sample, whereas the intermediate haplotypes are not observed at all. Bottom panel: a possible time evolution of how the haplotypes arose. Nodes without a number correspond to haplotypes which haven't appeared yet. At first one sequence is present, the ancestral sequence, which split into two (the first event is always a split, otherwise that haplotype would disappear). Then one of those two identical sequences may split again to give us a total of three (or could have mutated to give a new haplotype). One of those three then mutates to give us the intermediate haplotype, which in turn here splits and then mutates (and goes extinct) to give us the right-hand leaf. Finally, the intermediate haplotype mutates again to give us the left-hand leaf, which then also splits to give another copy of itself.

Simulating a temporal ordering implies that, starting with the ancestral sequence, we specify a series of split and mutation events which occurred by mimicking evolution, eventually resulting in the observed haplotype tree. A possible series of events is shown in Figure 10 through 7 timepoints, where node numbers indicate number of copies of each haplotype.

Notice that, if the root node had split further, we would have had three copies of the root haplotype. Although in theory this could have happened, with one of the copies eventually becoming extinct, we do not take into account any such scenarios, instead we only account for the observed sequences. Additionally, it would not have been possible for the intermediate haplotype to mutate after Step 3 above, since then it would disappear from the ancestral sequences, and another mutation would not have been possible.

7.2. Computational issues

Haplotype tree likelihood

When calculating the Metropolis-Hastings ratio for a proposal from root r to r' , one needs to

calculate

$$\frac{p(r' \mid T, \mathcal{S})}{p(r \mid T, \mathcal{S})} = \frac{\frac{|\mathcal{O}_{r',T}^{\mathcal{S}}|}{\sum_r |\mathcal{O}_{r,T}^{\mathcal{S}}|}}{\frac{|\mathcal{O}_{r,T}^{\mathcal{S}}|}{\sum_r |\mathcal{O}_{r,T}^{\mathcal{S}}|}} = \frac{|\mathcal{O}_{r',T}^{\mathcal{S}}|}{|\mathcal{O}_{r,T}^{\mathcal{S}}|}.$$

However, computing the size of the two sets of temporal orderings is a computational bottleneck. To overcome this issue, an unbiased estimator of the likelihood is used instead. Conditionally on a root r and tree T , a particular ordering O^* is generated by moving from the root to the tips and randomly choosing among the available split/mutate moves at each step, according to some distribution $q(O^*)$, such that any possible ordering of $\mathcal{O}_{r,T}^{\mathcal{S}}$ can arise. Then calculate

$$\widehat{|\mathcal{O}_{r',T}^{\mathcal{S}}|} = \frac{1}{q(O^*)},$$

such that

$$\mathbb{E} \left(\widehat{|\mathcal{O}_{r',T}^{\mathcal{S}}|} \right) = \sum_{O^* \in \mathcal{O}_{r,T}^{\mathcal{S}}} \frac{1}{q(O^*)} \times q(O^*) = |\mathcal{O}_{r',T}^{\mathcal{S}}|,$$

so it provides an unbiased estimator of the likelihood. Note here that the latent variable O is not accepted/rejected together with the root, so the Markov chain Monte Carlo does not maintain detailed balance (see [Manolopoulou and Emerson 2012](#); [Beaumont 2003](#)). This is because variance of $q(O^*)$ can be huge and detrimental to the MCMC, causing it to get ‘stuck’; future improvements of $q(O^*)$ could allow O^* to be accepted/rejected together with the root r . Multiple realizations of O^* could also be used instead, but **BPEC** only considers 1.

MCMC exploration and convergence

The **BPEC** model faces two additional key computational bottlenecks. The first comes from learning the posterior probability of the root haplotype. Since it relies upon an estimator of the likelihood, a large number of iterations are required in order to allow for reasonable convergence. However, the total number of haplotypes (and as such the number of possible roots) is generally low (usually up to a few hundreds), so with enough iterations the sampler can explore the whole root parameter space sufficiently.

On the other hand, the clustering parameter space is challenging to adequately explore. Instead, sophisticated local proposals are required. [Manolopoulou et al. \(2011\)](#) implement a clustering proposal which cumulatively adds observation branches (as shown in Figure 5) to clusters by starting with empty clusters with mean and variance equal to their corresponding prior means. As each observation branch is added to one of the clusters (in random order), the means and variances of that cluster are updated according to the corresponding posterior means. This allows the sampler to propose clusters for each branch according to the cluster in which it fits best, while randomising the order of the allocation meant that no branches were given higher weight than others. In **BPEC** we tweak the proposal distribution of [Manolopoulou et al. \(2011\)](#) by introducing an auxiliary variable w_c , representing the weight of the previous clustering in the MCMC sampler. Rather than simply allocating each

observation branch to one of the existing clusters simply by assessing the fit of each branch to each of the clusters, we assign it to the same cluster as the previous iteration (where possible) with probability w_c . This favours clusterings similar to the previous iteration, thereby ensuring that local moves are proposed more frequently. Since w_c is an auxiliary variable, it is accepted/rejected together with the proposed parameters, so the sampler automatically chooses a value of w_c that is reasonable.

Label-switching

In order to draw cluster-specific inferences, cluster labels need to be assigned for every posterior sample available. This is known as the label-switching problem (Stephens 2000a,b; Papastamoulis and Iliopoulos 2010) and it is especially challenging in the case of a variable number of clusters. Here we take a pivoting approach to assign cluster labels on-line (i.e., without the need of post-processing). The algorithm works as follows:

1. During burn-in of the first chain, record the cluster labels of the posterior sample with the highest value of the posterior density, denoted by \mathbf{c}^* .
2. Once this clustering is fixed, subsequent labels of the posterior sample of the set (μ, Σ) are chosen such that

$$p(\mathbf{Y} \mid \mu_{\mathbf{c}^*}, \Sigma_{\mathbf{c}^*}, \mathbf{c}^*)$$

is maximised. In other words, labels of the set of means and covariances are chosen such that the likelihood relative to (approximate) Maximum A Posteriori clustering \mathbf{c}^* is maximised.

Hashing

In contrast to coalescent trees, which are binary and can be represented simply by the pairs of subsequent coalescence events, haplotype trees do not have shorthand representations. Instead, a standard way to represent a haplotype tree is through its corresponding graph adjacency matrix. However, keeping track of posterior samples of trees requires storing entire matrices at each iteration of the sampler, which creates a memory bottleneck.

In our case, we can take advantage of the fact that not all adjacency matrices are possible; most edges are either certainly present or absent as determined by Ω . Uncertainty only arises through edges that are part of a loop in the network, so each tree is characterised by the set of deleted edges. Trees are then reduced to vectors of length n_{loop} with integer entries. Standard hashing techniques can thus be used to store the number of times each tree (i.e., each integer vector) appears in the MCMC posterior samples.

Hashing algorithms allow us to represent integer vectors by a single integer. In our case, we can store the index of the edge deleted from each loop at each iteration of the MCMC, keeping track of them via the ‘hashing index’ of the entire vector. Hash functions create a short (as short as possible) address book where each of these numbers is stored in a specific page, in such a way that it can easily be retrieved (see Knuth 1998).

Affiliation:

Ioanna Manolopoulou
Department of Statistical Science University College London
London WC1E 6BT, UK
E-mail: ioanna@stats.ucl.ac.uk
URL: <http://www.homepages.ucl.ac.uk/~ucakima/>

Axel Hille
Institute of Applied Statistics Dr. Jörg Schnitker Ltd.
Bielefeld
Germany
E-mail: axel.hille@gmx.net